

Dynamical Correlation Length and Relaxation Processes in a Glass Former

Raffaele Pastore,^{1,*} Massimo Pica Ciamarra,¹ Antonio de Candia,¹ and Antonio Coniglio¹

¹*CNR-SPIN, Dip.to di Scienze Fisiche, Università di Napoli "Federico II", Naples, Italy*

(Dated: Received: November 14, 2019/ Revised version:)

We investigate the relaxation process and the dynamical heterogeneities of the kinetically constrained Kob-Anderson lattice glass model, and show that these are characterized by different timescales. The dynamics is well described within the diffusing defect paradigm, which suggest to relate the relaxation process to a reverse-percolation transition. This allows for a geometrical interpretation of the relaxation process, and of the different timescales.

PACS numbers: 64.60.ah,61.20.Lc,05.50.+q

The hallmark of glass forming liquids, which is the rapid increase of the relaxation time as the temperature decreases [1], has been related to dynamical heterogeneities, growing spatio-temporal correlations in the dynamics. Dynamical heterogeneities are predicted by theories of the glass transition such as the mode-coupling theory, diffusing defects, and the random first order theory [2], and have been observed in both experimental and numerical studies [3]. These studies mostly focused on the dynamical susceptibility χ_4 , whose maximum value χ_4^* estimates the number of dynamically correlated particles. This maximum is expected to occur at a time close to the relaxation time τ , and to grow on approaching the transition of structural arrest, as frequently observed. However, there exist systems where χ_4^* is found to decrease on approaching the transition [4-6], as well as early studies suggesting that the time of maximal correlation between particles displacements does not scale with the relaxation time τ [7]. Accordingly, the relation between the dynamical susceptibility and the relaxation process remains elusive, and its clarification of great interest as it would allow to contrast different theories of the glass transition. Here we address this problem via a numerical study of the Kob-Anderson kinetically constrained lattice gas model [8], where it is possible to obtain very accurate data for the dynamical correlation length. We show that the relaxation process and the dynamical heterogeneities are characterized by two different timescales, which implies that they are less tangled than expected. We explain this feature in the diffusing defect picture, where we relate the relaxation process to a reverse percolation transition, and obtain a geometrical interpretation of the relaxation process and of the different timescales.

The Kob-Anderson lattice glass model [8] is a kinetically constrained model [9], in which a particle is allowed to move in a near empty site if has less than $m = 4$ neighbors, and if it will also have less than $m = 4$ neighbors after the move. Previous studies have shown that this model reproduces many aspects of the dynamics of glass forming systems, the slowing down of the dynamics on increasing the density suggesting the existence of a transition of structural arrest at $\rho_{ka} = 0.881$ [8, 10, 11], even

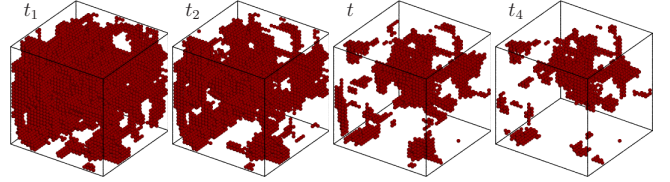


FIG. 1. (Color online) Persistent particles in a numerical simulations of the Kob-Anderson model at $\rho = 0.85$, at times $t_1 = 3.5 \cdot 10^5$, $t_2 = 7.5 \cdot 10^5$, $t_3 = 1.6 \cdot 10^6$, and $t_4 = 2.1 \cdot 10^6$.

though it has been demonstrated that in the thermodynamic limit the transition of dynamical arrest only occurs at $\rho = 1$ [12]. Here we investigate the relaxation process focusing on the time evolution of the density of persistent particles $p(t) = \frac{1}{V} \sum_{i=1}^V n_i(t)$, where $n_i(t) = 1(0)$ if site i is (is not) persistently occupied by a particle in the time interval $[0, t]$, and $\rho = N/V$ is the density. $p(t)$ is related to the high wave vector limit of the intermediate self scattering function [14]. As shown in Fig. 1, as time proceeds the density of persistent particles decreases, and spatial correlations between them emerge. These correlations are quantified by the dynamical susceptibility $\chi_4(t)$, related to the fluctuations of p ,

$$\chi_4(t) = \frac{V}{\rho} (\langle p(t)^2 \rangle - \langle p(t) \rangle^2), \quad (1)$$

and to the volume integral of the spatial correlation function between persistent particles at time t , $\chi_4(t) = \frac{1}{\rho V} \sum_{i,j}^V g_4(r, t)$, where

$$g_4(r, t) = \langle n_i(t)n_j(t) \rangle - \langle n_i(t) \rangle \langle n_j(t) \rangle, \quad r = |i - j|. \quad (2)$$

The spatial decay of $g_4(r, t)$ defines the dynamical correlation length $\xi(t)$.

Numerical results – We start by shortly summarizing our study of the dynamics of the KA model [13], which extends previous results and allows to obtain new insights on the glassy dynamics. The values of the exponents characterizing the dynamics are summarized in Table I. Numerical results for $p(t)/\rho$ and $\chi_4(t)$ are shown in Fig. 2. For $\rho \leq 0.85$, the decay of $p(t)$ is well described by the von Schweidler law, $\langle p \rangle / \rho = f_0 - (t/\tau)^b$,

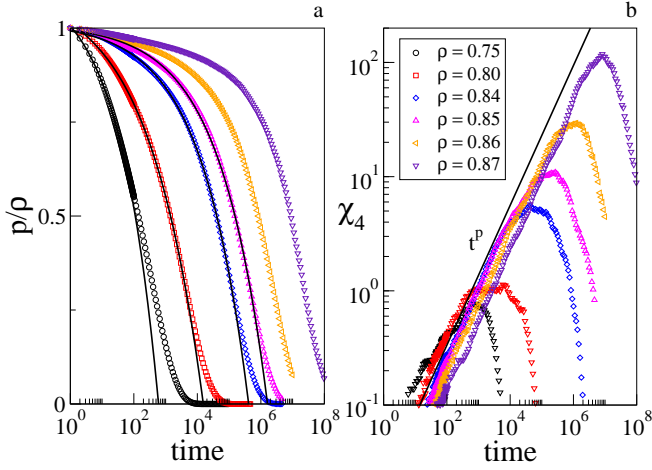


FIG. 2. (Color online) Normalized density of persistent particles $\langle p \rangle / \rho$ (panel a), and dynamical susceptibility χ_4 (panel b), for different values of the density, as indicated. For $\rho \leq 0.85$, $\langle p \rangle / \rho$ is well described by the von Schweidler law, $\langle p \rangle / \rho = f_0 - (t/\tau)^b$, with $f_0 = 1$ and $b \simeq 0.3$. At short times, the dynamical susceptibility grows as t^p , with $p \simeq 0.61$.

with $b \simeq 0.3$ and $f_0 \simeq 1$ in a large time window, while at higher densities b increases and f_0 decreases. The approach to the transition of structural arrest is marked by the increase of the relaxation time τ , we found to diverge as $\tau \propto (\rho_{ka} - \rho)^{-\lambda_\tau}$, as show in Fig. 3b, with $\lambda_\tau = 4.7 \pm 0.1$ consistent with previous results [8]. The emergence of an increasingly heterogeneous dynamics is signaled by the dynamical susceptibility, initially growing as $\chi_4(t) \propto t^p$, and then decreasing after reaching its maximum value χ_4^* at a time t_χ^* . The dynamical correlation length, which has a similar behavior, is illustrated in Fig. 3a, and is well described by

$$\xi(t) \propto t^a \exp(-at/t_\xi^*). \quad (3)$$

$\xi(t)$ grows as t^a at short times, and then decreases after reaching its maximum value ξ^* at time t_ξ^* , we find to diverge as $t_\xi^* \propto (\rho_{ka} - \rho)^{-\lambda_{t_\xi^*}}$, with $\lambda_{t_\xi^*} = 3.8 \pm 0.1$. The times τ and t_ξ^* diverge with different exponents as ρ approaches ρ_{ka} . This fact has rich consequences on the behavior of the susceptibility, we find to be well approximated by

$$\chi_4(t) \propto g(0, t)\xi(t)^{2-\eta} = p(t)(\rho - p(t))\xi(t)^{2-\eta}, \quad (4)$$

with $\eta \simeq 0$ [15]. Indeed, at low densities $t_\xi^* \gg \tau$, and Eq. 4 predicts $t_\chi^* \propto \tau$, while asymptotically $t_\chi^* \ll \tau$, and the maximum of the susceptibility χ_4^* occurs at $t_\chi^* \propto t_\xi^*$. Such a crossover in the behavior of t_χ^* is apparent in Fig. 3b. In addition, when $t_\chi^* \propto \tau$, the maximum of the susceptibility scales as $\chi_4^* \propto p(\tau)(\rho - p(\tau))\tau^{2a} \propto \tau^{2a} \propto (\rho_{ka} - \rho)^{-\gamma}$, with $\gamma = 2a\lambda_\tau$, in agreement with our results. Conversely, asymptotically $t_\chi^* \propto t_\xi^*$ and χ_4^* reflects the

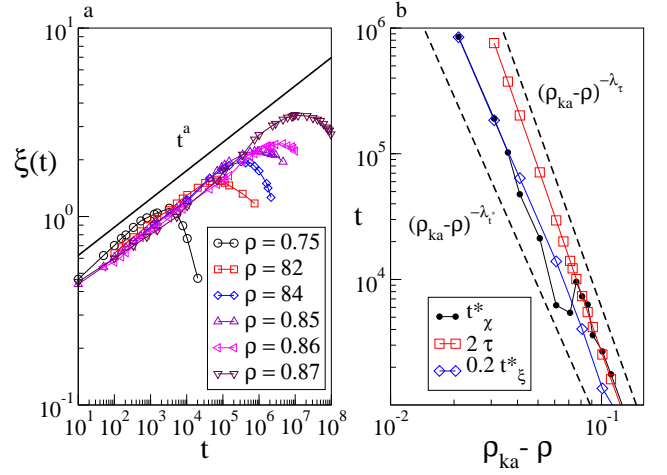


FIG. 3. (Color online) Panel a: dynamical correlation length for different values of the density. Panel b: divergence of the relaxation time τ , of the time where the correlation length acquires its maximum value t_ξ^* , and of the time where the dynamical susceptibility acquires its maximum value, t_χ^* . At low density, $t_\chi^* \propto \tau$, while at high density $t_\chi^* \propto t_\xi^*$. Errors on t_ξ^* and t_χ^* are of the order of 5%.

competition between the amplitude, which vanishes as $p(t_\xi^*)(\rho - p(t_\xi^*)) \propto (\rho_{ka} - \rho)^{-b(\lambda_{t_\xi^*} - \lambda_\tau)}$, and the correlation length, which diverges as $\xi^* \propto t_\xi^{*a} \propto (\rho_{ka} - \rho)^{-\nu}$, with $\nu = a\lambda_{t_\xi^*} \simeq 0.54$ (Fig. 4). Consequently $\chi_4^* \propto (\rho_{ka} - \rho)^{-q}$, with $q = b(\lambda_{t_\xi^*} - \lambda_\tau) + 2a\lambda_{t_\xi^*} \simeq 0.9$. Note that in other systems, where such decoupling between τ and t_ξ^* may occur with a negative q value, the susceptibility would decrease on approaching the transition of structural arrest, as observed in some experimental [4] and numerical [5, 6] studies.

The presence of a growing correlation length suggests that the system is approaching a critical point as the density increases. This scenario is conveniently described interpreting $\mu = -\log(t)$ as a chemical potential for the persistent particles, considering that the density of persistent particles monotonically decreases as time advances. The line where the correlation length reaches its maximum value in the μ - ρ plane can therefore be interpreted as a Widom line, which in a second order transition ends at the critical point. The results of Fig. 5 suggest the presence of a critical point located at $\rho = \rho_{ka}$ and $\mu = -\infty$, where the correlation length diverges. The Widom line will actually eventually bend, and end at $\rho = 1$ where the transition is known to occur in the thermodynamic limit. Such an approach may open the way to a renormalization group treatment of the glass transition.

Diffusing defects – The results described so far are rationalized in the diffusion defects paradigm [2, 16, 17], where the relaxation is ascribed to the presence of possibly extended diffusing defects, with density ρ_d . The

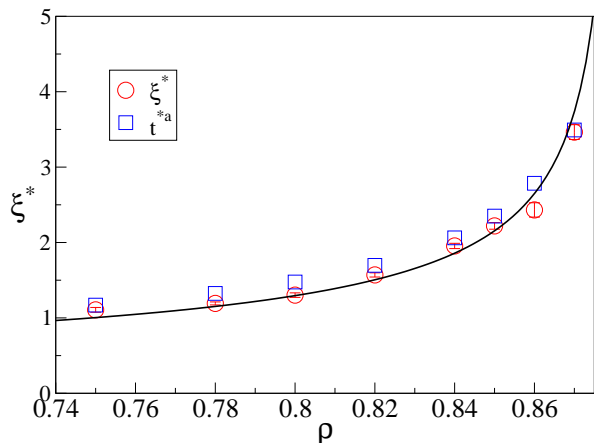


FIG. 4. (Color online) Dynamical correlation length at $t = t^*$, and prediction of the diffusing defect picture, $\xi^* \propto t^{*a} \propto \tau^a$, $q = a\lambda_\tau/\lambda_{t_\xi^*}$. The full line is a $(\rho_{ka} - \rho)^{-\nu}$, $\nu \simeq 0.54$ (we fix $\rho_{ka} = 0.881$ as estimated from the divergence of the relaxation time).

number of distinct sites visited by a defect grows as $n_v(t) \propto t^b$, while its mean square displacement grows as t^{2a} , $d_f = b/a$ being the defect fractal dimension. At short times, before defects interact, the persistence decays as $1 - p(t)/\rho \propto \rho_d n_v(t) \propto \rho_d t^b$, and therefore this picture reproduces the von Schweidler law, and relates the density of defects ρ_d with relaxation time, $\rho_d \propto \tau^{-b}$. The correlation length is expected to grow as t^a as long as different defects do not interact, since only sites visited by the same defect are correlated. Due to their subdiffusive nature, we expect defects to behave as random walkers characterized by a fat-tail waiting time distribution [18], which does not affect their fractal dimensions. The value of the fractal dimension is also largely unaffected by the possible presence of spatial correlations [19]. Accordingly, the diffusing defect picture predicts $b/a = d_f = 2$, in agreement with the numerical findings. This picture also predicts that the susceptibil-

exponent	measure	prediction
$p(t) = \rho(1 - (t/\tau)^b)$	$b = 0.3$	–
$\xi(t) \propto t^a$	$a = 0.156$	$a = b/2 = 0.15$
$\chi_4(t) \propto t^p$	$p = 0.6$	$p = 2b = 0.6$
$\tau \propto (\rho_{ka} - \rho)^{-\lambda_\tau}$	$\lambda_\tau = 4.7$	–
$t_\xi^* \propto (\rho_{ka} - \rho)^{-\lambda_{t_\xi^*}}$	$\lambda_{t_\xi^*} = 3.8$	–
$\xi^* \propto (\rho_{ka} - \rho)^{-\nu}$	$\nu = 0.54$	$\nu = a\lambda_{t_\xi^*} = 0.57$
$\chi_4^* \propto (\rho_{ka} - \rho)^{-\gamma}$	$\gamma = 1.43$	$\gamma = 2a\lambda_\tau = 1.41$ ($t_\xi^* \gg \tau$)

TABLE I. Exponents characterizing the slow dynamics of the KA model, and their relations according to the diffusing defects picture. The fractal dimension is $d_f = b/a$. The dynamics is characterized by three exponents, b , λ_τ and $\lambda_{t_\xi^*}$.

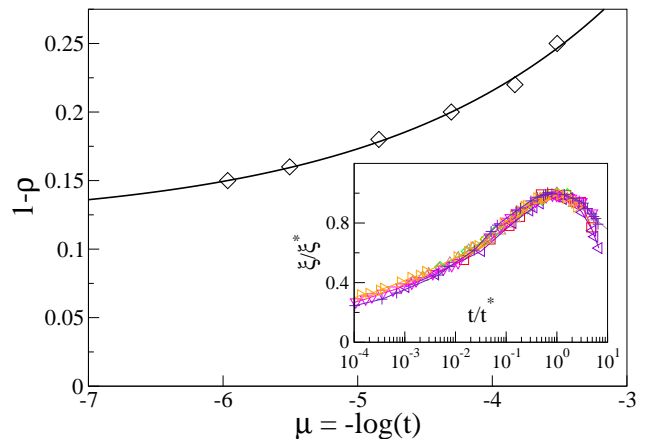


FIG. 5. (Color online) Main panel: Widom line in the density, chemical potential plane. Circles indicate the time t_ξ^* where the correlation length reaches its maximum value, at each value of the density. The continuous line corresponds to $(1 - \rho_{ka}) \propto (t/t^*)^{a/\nu}$, and suggests that the system approaches a critical point at $\mu = -\infty$, and $\rho = \rho_{ka}$. Inset: scaling of the dynamical susceptibility for 7 values of the density, in the range 0.78–0.87.

ity grows as the square of the number of sites visited by each defect [2], $\chi_4(t) \propto \rho_b n_v(t)^2 \propto t^{2b}$, which allows to correctly estimate $p = 2b$.

Reverse percolation – As time advances defects induce a reverse percolation transition of persistent particles, clearly visible in Fig. 1, which is similar to the gradual destruction of a polymer gel through diffusing enzymes [20, 21]. Since the absence of a percolating cluster of persistent particles leads to the loss of mechanical rigidity on all timescales, this transition is related to the relaxation process. Indeed, the study of the density of the percolating cluster P , reveals that the percolation time scales with the relaxation time, as shown in Fig. 6. The figure also reveals that P equals p up to large times, which implies that the density of finite clusters $p-P$ is negligible during most of the relaxation process. At large times, finite clusters appear and have a broad size distribution, and consequently different relaxation timescales, thus explaining the crossover in decay of $p(t)$, which is first described by a power-law, and then by a stretched exponential. Fig. 6 also shows that the dynamical correlation length coincides with the percolative length extracted from the pair connected correlation function [22], as long as finite clusters are negligible. The percolative length is affected by the two timescales characterizing the glassy dynamics, the time $t = t_\xi^*$ where the dynamical length reaches its maximum value, and the percolating time related to the relaxation of the system. At high densities, this makes ξ_{per} non monotonic, as in Fig. 6.

Future directions – Our results suggest that in the KA model the relaxation dynamics and the dynamical het-

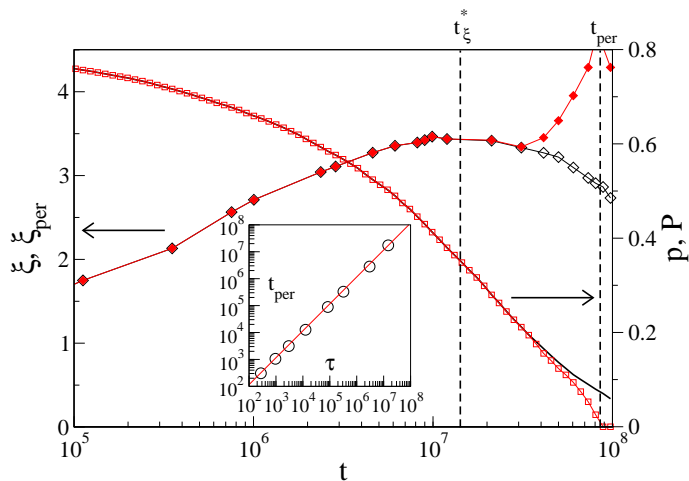


FIG. 6. (Color online) Percolation transition at $\rho = 0.87$. Left axis: dynamical correlation length ξ (empty diamonds) and percolation correlation length ξ_{per} (full diamonds). Right axis: density of persistent particles $\langle p \rangle$ (full line) and strength of the percolating cluster $\langle P \rangle$ (squares). The vertical dashed lines mark t_ξ^* and t_{per} , which is proportional to τ (inset).

erogeneities are characterized by different timescales, τ and t_ξ^* . This may be explained considering that τ occurs when a given large fraction of all sites has relaxed, while t_ξ^* occurs when the correlations between the persistent particles decreases. In principle, these correlations may decrease before a large fraction of all sites has relaxed. Since $\tau \propto t_\xi^*$ when defects behave as perfect random walkers [2], one may speculate that the decoupling between the two timescales may be due to a more complex nature of defects, such as the non conservation of defects characterized by birth and death rate with a constant average number or the presence of heterogeneous defects. Future plans include the study of the dynamical correlation length in off-lattice models of glass forming liquids, to verify the possible existence of different timescales.

* pastore@na.infn.it

- [1] C.A. Angell, Science **267**, 1924 (1995). M.D. Ediger, C.A. Angell and S.R. Nagel, J. Phys. Chem. **100**, 13200 (1996). P.G. Debenedetti and F.H. Stillinger, Nature **410**, 259 (2001). G.Adam and J.H. Gibbs, J. Chem. Phys. **43**, 139 (1965).
 [2] C. Toninelli, M. Wyart, L. Berthier, G. Biroli and J.-P.

- Bouchaud, Phys. Rev. E **71**, 041505 (2005).
 [3] M.D. Ediger, Annu. Rev. Phys. Chem. **51**, 99.(2000). M.M. Hurley, P. Harrowel, Phys. Rev. E **52**, 2 (1995). S. Franz and G. Parisi, J. Phys. Condens. Matter **12**, 6335 (2000). C. Donati, S. Franz, G. Parisi, and S. C. Glotzer, J. Non-Cryst. Solids **307**, 215 (2002). E. Weeks, J. C. Crocker, A. C. Levitt, A. Schofield, and D. A. Weitz, Science **287**, 627 (2000).
 [4] P. Ballesta, A. Duri and L. Cipelletti, Nature Physics **4**, 550 (2008).
 [5] S. C. Glotzer, V. N. Novikov and T. B. Schrøder J. Chem. Phys. **112**, 509 (2000).
 [6] A. Fierro, A. de Candia and A. Coniglio, Phys. Rev. E **62**, 7715 (2000).
 [7] S.C. Glotzer and Claudio Donati J. Phys.: Condens. Matter **11**, A285 (1999).
 [8] W. Kob and H.C. Andersen, Phys. Rev. E **48**, 4364 (1993).
 [9] F. Ritort and P. Sollich, Advances in Physics **52**, 219 (2003) and references therein.
 [10] S. Franz, R. Mulet and G. Parisi, Phys. Rev. E **65**, 021506 (2002).
 [11] A. Lawlor, D. Reagan, G.D. McCullagh, P. De Gregorio, P. Tartaglia, and K.A. Dawson, Phys. Rev. Lett. **89**, 245503 (2002).
 [12] C. Toninelli, G. Biroli, D.S. Fisher, Phys. Rev. Lett **92**, 18 (2004).
 [13] We have performed Monte Carlo simulations of the standard Kob–Andersen (KA) model in three dimensions [8], for $L = 30$, performing up to 10^8 sweeps. For each value of the density, we have averaged our results over up to 10^4 runs.
 [14] D. Chandler, J.P. Garrahan, R.L. Jack, L. Maibaum and A.C. Panel, Phys. Rev. E **74**, 051501 (2006).
 [15] L. Berthier, G. Biroli, J.-P. Bouchaud and R. L. Jack, in *Dynamical heterogeneities in glasses, colloids, and granular media*, Eds.: L. Berthier, G. Biroli, J-P Bouchaud, L. Cipelletti and W. van Saarloos (Oxford University Press, to appear) arXiv:1009.4765v2.
 [16] L. Berthier and G. Biroli, arXiv:1011.2578 (2010).
 [17] J.T. Bendler and M.F. Shlesinger, Journal of Statistical Physics **53**, 531 (1988).
 [18] S.B. Yuste, J. Klafter, and K. Lindenberg, Phys. Rev. E **77**, 032101 (2008).
 [19] A. Ordemann, G. Berkolaiko, S. Havlin, and A. Bunde, Phys. Rev. E **61**, R1005 (2000).
 [20] T. Abete, A. de Candia, D. Lairez and A. Coniglio, Phys. Rev. Lett. **93**, 228301 (2004).
 [21] V. Sidoravicius and A. S. Sznitman, Comm. Pure Appl. Math. **62**, 831 (2009).
 [22] The pair connected correlation function can be expressed as $g_{pc}(r) - P^2 = P_{ij}^f(r) + (P_{ij}^\infty(r) - P^2)$, where P_{ij}^f and P_{ij}^∞ are the probabilities that two sites i and j occupied by persistent particles belong to a same finite cluster, or to the infinite cluster, respectively. See A. Coniglio A and R. Figari, J. Phys. A: Math. Gen. **16** L535 (1983).